Annals of Internal Medicine ORIGINAL RESEARCH

Association Between Body Composition and Cardiometabolic Outcomes

A Prospective Cohort Study

Matthias Jung, MD; Marco Reisert, PhD; Hanna Rieder; Susanne Rospleszcz, PhD; Michael T. Lu, MD, MPH; Fabian Bamberg, MD, MPH; Vineet K. Raghu, PhD*; and Jakob Weiss, MD*

Background: Current measures of adiposity have limitations. Artificial intelligence (AI) models may accurately and efficiently estimate body composition (BC) from routine imaging.

Objective: To assess the association of AI-derived BC compartments from magnetic resonance imaging (MRI) with cardiometabolic outcomes.

Design: Prospective cohort study.

Setting: UK Biobank (UKB) observational cohort study.

Participants: 33 432 UKB participants with no history of diabetes, myocardial infarction, or ischemic stroke (mean age, 65.0 years [SD, 7.8]; mean body mass index [BMI], 25.8 kg/m^2 [SD, 4.2]; 52.8% female) who underwent whole-body MRI.

Measurements: An AI tool was applied to MRI to derive 3-dimensional (3D) BC measures, including subcutaneous adipose tissue (SAT), visceral adipose tissue (VAT), skeletal muscle (SM), and SM fat fraction (SMFF), and then calculate their relative distribution. Sex-stratified associations of these relative compartments with incident diabetes mellitus (DM) and major adverse cardiovascular events (MACE) were assessed using restricted cubic splines.

Results: Adipose tissue compartments and SMFF increased and SM decreased with age. After adjustment for age, smoking, and hypertension, greater adiposity and lower SM proportion were associated with higher incidence of DM and MACE after a median follow-up of 4.2 years in sex-stratified analyses; however, after additional adjustment for BMI and waist circumference (WC), only elevated VAT proportions and high SMFF (top fifth percentile in the cohort for each) were associated with increased risk for DM (respective adjusted hazard ratios [aHRs], 2.16 [95% CI, 1.59 to 2.94] and 1.27 [CI, 0.89 to 1.80] in females and 1.84 [CI, 1.48 to 2.27] and 1.84 [CI, 1.43 to 2.37] in males) and MACE (1.37 [CI, 1.00 to 1.88] and 1.72 [CI, 1.23 to 2.41] in females and 1.22 [CI, 0.99 to 1.50] and 1.25 [CI, 0.98 to 1.60] in males). In addition, in males only, those in the bottom fifth percentile of SM proportion had increased risk for DM (aHR for the bottom fifth percentile of the cohort, 1.96 [CI, 1.45 to 2.65]) and MACE (aHR, 1.55 [CI, 1.15 to 2.09]).

Limitation: Results may not be generalizable to non-Whites or people outside the United Kingdom.

Conclusion: Artificial intelligence–derived BC proportions were strongly associated with cardiometabolic risk, but after BMI and WC were accounted for, only VAT proportion and SMFF (both sexes) and SM proportion (males only) added prognostic information.

Primary Funding Source: None.

Ann Intern Med. doi:10.7326/ANNALS-24-01863
For author, article, and disclosure information, see end of text.
This article was published at Annals.org on 30 September 2025.
* Drs. Raghu and Weiss jointly supervised this work.

Obesity is a global epidemic that is estimated to have caused 4 million deaths in 2015, primarily driven by excess cardiometabolic disease (1). Forty percent of the global population has overweight or obesity, and it is projected that more than 60% of U.S. adults will have obesity by 2050 (1, 2). Current obesity definitions rely on body mass index (BMI) (>25 to <30 kg/m^2 for overweight and ≥30 kg/m^2 for obesity); however, this conflates excess adiposity with muscle mass and does not account for the location of body fat, which is a critical factor in the assessment of obesity-related cardiometabolic risk (3). Alternative definitions using waist circumference (WC), anthropometric measures, or dual-energy x-ray absorptiometry may allow more direct assessment of adiposity but still cannot differentiate fat location and distribution (for example, visceral adipose tissue [VAT] vs. subcutaneous adipose tissue [SAT]) (4–6).

Cross-sectional scans, such as magnetic resonance imaging (MRI) and computed tomography (CT), have the potential to improve adiposity assessment, as their availability and use are increasing, with an 86% increase in MRI volume and a 127% increase in CT volume in England over the past decade (7, 8) and approximately 36 million MRI scans and 85 million CT scans performed in the United States in 2021 (9, 10). Despite the well-

See also:
Web-Only
Supplement

established link between adiposity and muscle with cardiometabolic and other diseases (9–11), body composition (BC) measures derived from MRI and CT are not currently quantified in daily practice (11–13). Advances in artificial intelligence (AI) have enabled automated, efficient 3-dimensional (3D) segmentation of BC compartments, which are more strongly associated with mortality than surrogate 2D areas (14). However, the relationship between imaging-derived BC volumes and cardiometabolic outcomes is unknown.

In this study, we used an open-source AI model to estimate 3D BC volumes, including SAT, VAT, skeletal muscle (SM), and SM fat fraction (SMFF), from whole-body MRIs of more than 30 000 people from the UK Biobank (UKB). We calculated relative adiposity and muscle (for example, relative SAT is the ratio of SAT to total SAT, VAT, and SM volume) to control for disease-independent factors like sex and height that affect total body size (10, 15). Finally, we assessed age- and sex-specific distributions of relative BC compartments across the lifespan and investigated the association between relative BC measures and future cardiometabolic disease risk (diabetes mellitus [DM] and major adverse cardiovascular events [MACE]) beyond BMI, WC, and other traditional risk factors.

METHODS

Data Source

This study used data from the UKB, a large population-based cohort study of the general population (16, 17). Between 2006 and 2010, 500 000 people aged 40 to 69 years (5.5% of invitees) joined the UKB at the invitation of the National Health Service (18). A subgroup of participants has undergone a panel of imaging studies, including MRI. At the MRI appointment, participants also completed a questionnaire and underwent anthropometric measurements. All surviving UKB participants are invited to participate in this substudy, except those who no longer wish to be contacted or now live outside the United Kingdom. The MRI protocol includes a whole-body T_1-weighted 3D-VIBE 2-point Dixon sequence. Dixon MRI separates the MRI signals of water and fat, allowing accurate fat and muscle tissue segmentation. Further information is provided in the **Supplement Methods** (available at Annals.org). An overview of our study design is provided in **Supplement Figure 1** (available at Annals.org), and a flowchart is shown in **Supplement Figure 2** (available at Annals.org).

Deep-Learning Model and BC Measures

We used a validated deep-learning (DL) model to measure SAT, VAT, and SM (volumes) and SMFF (percentage) from whole-body MRI (14). In brief, the model was trained on 150 random participants from the German National Cohort (NAKO; whole-body 3-Tesla Dixon MRI) (19); SAT, VAT, and SM were manually annotated by a radiology resident (5 years of experience in MRI) using a semiautomatic threshold-based 3D segmentation tool in an open-source imaging platform (https://www.nora-imaging.org). Initial segmentations were reviewed by a board-certified attending radiologist (10 years of experience in MRI) and flagged if errors were noted. Flagged examinations were resolved by consensus between the radiology resident and the attending radiologist, and segmentations were corrected when necessary (minor adjustments were made in about 10% of cases).

After training, the model was tested on 50 independent manually segmented NAKO test MRIs not seen during training. These served as ground truth to assess model performance using Dice scores, which measure segmentation accuracy from 0 to 1, with 1 representing perfect overlap between predicted and manual ground-truth segmentations. In our previous study, we reported high agreement between automatic and manual segmentations in the testing data set, with Dice scores of 0.95 ± 0.02 for SAT, 0.92 ± 0.03 for VAT, and 0.93 ± 0.02 for SM (14). We retrained the model using a random sample of 130 UKB MRIs, allowing the model to learn nuances (fine-tuning) between the 1.5-Tesla and 3-Tesla Dixon MRIs used in NAKO. After fine-tuning, we reported Dice scores of 0.93 ± 0.01 for SAT, 0.90 ± 0.01 for VAT, and 0.90 ± 0.03 for SM on the UKB testing set ($n = 50$) (14).

Here, we provide Bland–Altman plots to test the model performance in the UKB (**Supplement Figure 3**, available at Annals.org). Bland–Altman plots showed good agreement between manual and DL-based segmentations. For SAT, the mean difference was −0.22 L (limits of agreement, −1.42 to 0.98 L), indicating a slight underestimation of SAT (cohort median, 14.9 L [IQR, 11.6 to 19.3 L]; **Table**) by the DL model (**Supplement Figure 3A**, available at Annals.org). Visceral adipose tissue had a mean difference of 0.37 L, with differences tightly clustered around the mean (limits of agreement, 0.03 to 0.72 L), reflecting slight overestimation of VAT (cohort median, 3.4 L [IQR, 2.0 to 5.3 L]; **Table**) but strong concordance (**Supplement Figure 3B**, available at Annals.org). Skeletal muscle showed a mean difference of 0.5 L, with slightly more variability but overall consistent agreement (limits of agreement, −0.36 to 1.36 L [**Supplement Figure 3C**, available at Annals.org]; cohort mean, 11.4 [SD, 3.0] [**Table**]). Sample segmentation results illustrating the model's performance across BMI categories and sex are shown in **Supplement Figure 4** (available at Annals.org).

In addition, we quantified the SMFF, a marker of muscle quality that captures metabolically active intramyocellular fat that is not macroscopically visible. The SMFF can be estimated from Dixon MRI, which allows for voxel-wise extraction of water and fat signals, enabling calculation of a fat fraction (fat signal / [fat + water signal]) from BC segmentation masks. A common drawback of Dixon MRI is "swap artifacts," where fat signals are misrepresented as water signals, leading

Table. Cohort Characteristics

Characteristic	Overall (*n* = 33 432)	Female (*n* = 17 657)	Male (*n* = 15 775)
White race, *n (%)*	33 432 (100)	17 657 (100)	15 775 (100)
Age, *y*			
Mean (SD)	65.0 (7.8)	64.4 (7.6)	65.6 (7.9)
Median (IQR)	65.4 (59.0–71.0)	64.6 (58.5–70.3)	66.4 (59.6–71.8)
BMI, *n (%)*			
<25 kg/m^2	16 022 (48)	9708 (55)	6314 (40)
25–29.9 kg/m^2	12 657 (38)	5474 (31)	7183 (46)
≥30 kg/m^2	4753 (14)	2475 (14)	2278 (14)
Waist circumference, *cm*			
Mean (SD)	88.1 (12.5)	82.6 (11.6)	94.2 (10.5)
Median (IQR)	88.0 (79.0–96.0)	81.0 (74.0–90.0)	93.0 (87.0–100.0)
Median SAT volume (IQR), *L*	14.9 (11.6–19.3)	17.0 (13.4–21.6)	13.0 (10.4–16.3)
Median VAT volume (IQR), *L*	3.4 (2.0–5.3)	2.4 (1.4–3.6)	5.0 (3.4–6.6)
Mean SM volume (SD), *L*	11.4 (3.0)	9.1 (1.3)	14.0 (2.1)
Mean SMFF (SD), %	16.0 (3.2)	17.1 (3.0)	14.7 (2.9)
History of hypertension, *n (%)*	4293 (13)	1852 (10)	2441 (15)
Smoking status, *n (%)**			
Never	15 431 (47)	8671 (50)	6760 (43)
Former	17 023 (51)	8478 (49)	8545 (55)
Current	634 (1.9)	297 (1.7)	337 (2.2)
Incident diabetes mellitus, *n (%)*	531 (1.6)	187 (1.1)	344 (2.2)
Incident MACE, *n (%)*	542 (1.6)	177 (1.0)	365 (2.3)
Follow-up time, *y*			
Mean (SD)	4.5 (1.8)	4.5 (1.8)	4.4 (1.8)
Median (IQR)	4.2 (3.3–5.6)	4.2 (3.4–5.6)	4.2 (3.3–5.5)

BMI = body mass index; MACE = major adverse cardiovascular events; SAT = subcutaneous adipose tissue; SM = skeletal muscle; SMFF = skeletal muscle fat fraction; VAT = visceral adipose tissue.
* *n* = 33 088 for smoking status.

to incorrect fat fraction calculations. Swap artifacts occurred in raw scan regions, such as the abdomen, where, for example, fat was incorrectly displayed as water contrast. When fat and water images were stitched into a whole-body MRI, this swapping caused some regions, such as the abdomen, to be displayed incorrectly (for example, as water contrast), whereas other regions, such as the chest and pelvis, remained correctly displayed as fat contrast. Therefore, we used a second open-source model to correct for these region-wise swaps in the stitched whole-body MRIs before SMFF quantification, as reported elsewhere (14). Briefly, the model was tested on 180 whole-body MRIs with swaps, and performance was verified by visual review from the radiology resident. All swaps were accurately corrected.

Outcomes

Primary outcomes were incident DM (International Classification of Diseases, 10th Revision [ICD-10] codes E10 to E14 or ICD-9 code 250) and MACE, defined as myocardial infarction or ischemic stroke (ICD-10 codes I21 to I22, I63, or I00 to I78 or ICD-9 codes 410 to 411 or 433 to 434) or mortality from major cardiovascular diseases (ICD-10 codes I1 to I6 or I70 to I78). Outcomes were defined using UKB Data Fields 41270 and 41271, which contain distinct ICD-9 and ICD-10 diagnosis codes through linkage to all hospital inpatient records (https://biobank.ctsu.ox.ac.uk/crystal/refer.cgi?id=138483). Mortality from major cardiovascular diseases was extracted through linkage to national death registries (Data Field 40001). Follow-up time was calculated as the interval between the date of MRI (start and origin time) and death, occurrence of an outcome, loss to follow-up, or 31 October 2022 (the censoring date for ICD-based outcomes), whichever occurred first.

Covariates

Date of birth, sex, and race were extracted from baseline self-reports. Weight (in kilograms), height (in meters), and WC (in centimeters) were obtained at the imaging visit. Body mass index (in kilograms divided by the square of height in meters) was categorized as healthy weight (<25 kg/m^2), overweight (25 to 29.9 kg/m^2), or obesity (≥30 kg/m^2). Body mass index below 18 kg/m^2 was included in the healthy weight group due to underrepresentation ($n = 230$). Smoking was categorized as "never," "former," or "current." Prevalent hypertension was defined as presence of ICD-10 codes I10 to I15 or ICD-9 codes 401 to 405 before the imaging visit. Non-Whites ($n = 1193$ [3% in the UKB]) were excluded due to substantial heterogeneity in the association of BC with disease across ethnic groups and inadequate sample sizes to support robust ethnicity-specific analyses. Covariates were identified using a modified disjunctive cause criterion.

Statistical Analysis

Baseline characteristics are presented as means and SDs or medians with IQRs for continuous variables and as absolute counts with percentages for categorical variables.

After automatic extraction of SAT, VAT, and SM, we defined relative BC compartments to adjust for disease-independent contributors to SAT, VAT, and SM volumes, such as sex or body size. Relative compartments were defined as the ratio of each measure to the sum of all BC measures; for example, SAT_{rel} was equal to SAT / (SAT + VAT + SM). A SAT_{rel} of 60% indicates that 60% of a person's total adiposity and muscle is SAT, with the remaining 40% comprising VAT and SM. Differences in relative BC compartments and SMFF across ages were visualized using density plots.

Outcome analyses were limited to people with no history of DM, myocardial infarction, or ischemic stroke. To investigate time to outcome, sex-stratified restricted cubic splines (natural splines) with 2 degrees of freedom were computed using the splines package (version 4.4.2) in R. We calculated sequential models to assess the association between relative BC measures and outcomes, with a model adjusted only for age, smoking, and hypertension and a model additionally adjusted for BMI categories and WC. Results were also reported as adjusted hazard ratios (aHRs) and 95% CIs for the top and bottom 5% and 20% of males and females,

respectively. For the underlying sex-stratified Cox models, proportional hazards assumptions were tested by computing scaled Schoenfeld residuals, and linearity was assessed using martingale residuals. Both assumptions were met for all models. Cox regressions were complete-case analyses that excluded people with 1 or more missing covariates.

Statistical analyses were performed using R, version 4.2.2 (R Foundation for Statistical Computing [www.r-project.org]).

Role of the Funding Source

This study received no funding.

RESULTS

Study Population and BC Distribution by Age

A total of 33 432 people (17 657 females; mean age, 65.0 years [SD, 7.8]; mean BMI, 25.8 kg/m^2 [SD, 4.2]) were included. The **Table** presents baseline characteristics of included participants. Females had higher SAT and SMFF than males, whereas males had higher SM and VAT ($P < 0.001$ for all; **Table**).

Across all age groups, SAT was the predominant compartment in females, comprising 58.1% of total BC at age 40 to 49 years and increasing to 60.1% above age 70 years compared with 40.0% and 41.5%, respectively, in males (**Figure 1**). Skeletal muscle was the predominant compartment in males, peaking at age 40 to 49 years (45.3% in males vs. 35.5% in females) and decreasing thereafter. In both sexes, VAT proportion and SMFF were also higher with increased age.

Relative BC Measures and Incident DM and MACE

Over a median follow-up of 4.2 years (IQR, 3.3 to 5.6 years), 187 (1.1%) of 17 657 females and 344 (2.2%) of 15 775 males were diagnosed with incident DM, and there were 177 (1.0%) and 365 (2.3%) MACE, respectively. **Figures 2** and **3** show results for the sex-stratified association of relative BC measures and future risk for DM and MACE after adjustment for age, smoking status, and hypertension and with additional adjustment for BMI categories and WC.

In models adjusted for age, smoking, and hypertension, greater adiposity measures (SAT proportion, VAT proportion, and SMFF) and low SM proportion were associated with higher incidence of DM and MACE in both sexes (**Figures 2** and **3** [upper rows]). These relationships were consistent with those in unadjusted analyses (**Supplement Figures 5** and **6**, available at Annals.org).

After additional adjustment for BMI and WC, the associations between SAT proportion and DM and MACE were attenuated in males (**Figure 2** [*B*] and **Figure 3** [*B*], lower rows), while we observed a negative association between relative SAT and future diabetes risk in females. Females in the bottom 20th percentile of relative SAT (<54.4%) had an aHR of 1.46 (95% CI, 1.23 to 1.72), while females in the top 20th percentile (>64.6%) had an aHR of 0.71 (CI, 0.59 to 0.84) (**Figure 2** [*A*], lower row).

In both sexes, high VAT proportions and high SMFF remained associated with higher risk for DM and MACE. For DM, aHRs for the top fifth percentile were 2.16 (CI, 1.59 to 2.94) and 1.27 (CI, 0.89 to 1.80) in females (**Figure 2** [*A*]) and 1.84 (CI, 1.48 to 2.27) and 1.84 (CI, 1.43 to 2.37) in males (**Figure 2** [*B*]), respectively. For MACE, aHRs were 1.37 (CI, 1.00 to 1.88) and 1.72 (CI, 1.23 to 2.41) in females (**Figure 3** [*A*]) and 1.22 (CI, 0.99 to 1.50) and 1.25 (CI, 0.98 to 1.60) in males (**Figure 3** [*B*]), respectively.

In males only, low SM proportions remained associated with increased risk for DM (aHR for bottom fifth percentile, 1.96 [CI, 1.45 to 2.65]; **Figure 2** [*B*]) and MACE (aHR for bottom fifth percentile, 1.55 [CI, 1.15 to 2.09]; **Figure 3** [*B*]) after adjustment for BMI and WC.

Results were consistent across BMI subgroups (**Supplement Figures 7 to 9**, available at Annals.org).

DISCUSSION

Excess adiposity is a key driver of cardiometabolic disease, but current definitions of obesity rely on BMI, an accessible but poor surrogate (3). In this study, we applied an AI segmentation tool to whole-body MRIs from more than 30 000 UKB participants to extract 3D BC compartments and estimate the relative proportion of SAT, VAT, SM, and SMFF. We found that the tool accurately extracted 3D BC volumes from whole-body MRIs in less than 3 minutes per scan and demonstrated that as both sexes age, adipose tissue compartments and SMFF increase while SM decreases. Before adjustment for BMI and WC, we found that greater adiposity and low SM proportion were associated with higher incidence of DM and MACE in both sexes in models adjusted for age, smoking, and hypertension. However, after BMI and WC were accounted for, only VAT proportion and SMFF were associated with incident DM and MACE in both sexes, whereas low SM proportion was associated with higher risk in males only.

These results corroborate evidence that VAT, but not SAT, is a key driver of adiposity-related cardiometabolic risk (20–22). Our results also support findings that ectopic fat in muscle leads to insulin resistance and cardiovascular risk (23, 24). Contrary to emerging evidence, we found that low SM proportions were more strongly associated with cardiometabolic risk in men than in women (25). Counterintuitively, we found that women with high SAT proportions had lower risk for incident DM after adjustment for BMI and WC. Subcutaneous adipose tissue may confer metabolic protection compared with visceral fat, particularly in women (26, 27). However, this seemingly protective association may simply reflect the inverse relationship between SAT and VAT proportions.

Body mass index has known limitations (28–31) and is only recommended as a population-based measure

Figure 1. Change in relative body composition across decades of age.

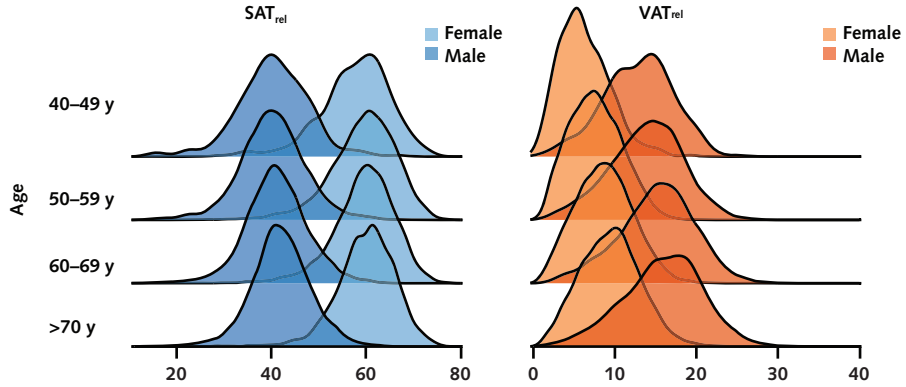

Age	Median SAT_{rel} (IQR), %		Median VAT_{rel} (IQR), %	
	Female	Male	Female	Male
40–49 y	58.1 (53.5–62.4)	40.0 (35.7–44.8)	5.6 (3.8–8.0)	13.1 (10.0–15.5)
50–59 y	59.7 (55.1–63.8)	39.9 (35.6–44.1)	7.3 (5.0–9.8)	13.9 (10.7–16.8)
60–69 y	59.8 (55.6–63.6)	40.6 (36.7–44.7)	8.4 (6.0–10.9)	15.2 (12.1–18.1)
>70 y	60.1 (56.1–63.8)	41.5 (37.9–45.5)	9.3 (6.6–11.7)	16.0 (12.6–19.0)

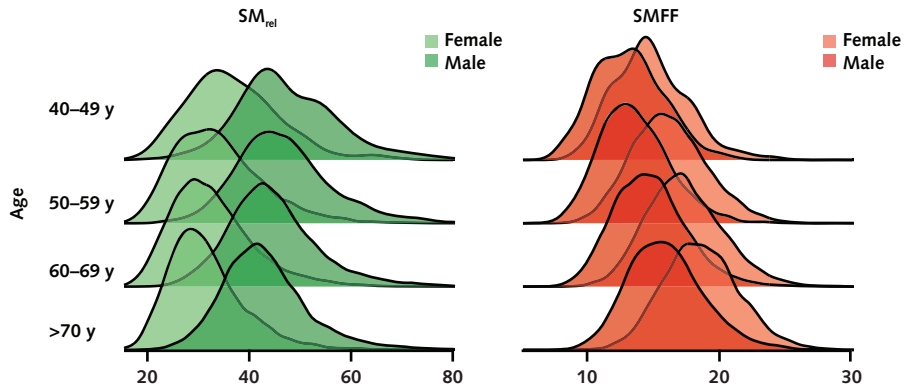

Age	Median SM_{rel} (IQR), %		Median SMFF (IQR), %	
	Female	Male	Female	Male
40–49 y	35.5 (30.2–41.7)	45.3 (40.7–53.3)	14.5 (12.8–16.3)	12.9 (11.1–14.6)
50–59 y	32.4 (27.1–38.3)	45.4 (40.1–51.5)	15.8 (14.0–17.9)	13.2 (11.5–15.1)
60–69 y	31.2 (26.5–36.6)	43.2 (38.4–48.9)	17.0 (15.2–19.0)	14.4 (12.6–16.3)
>70 y	29.9 (25.8–34.9)	41.7 (36.9–47.2)	18.4 (16.5–20.3)	15.6 (13.8–17.6)

The density plots illustrate the change in relative body composition measures (SAT_{rel} [*blue*], VAT_{rel} [*orange*], SM_{rel} [*green*], and SMFF [*red*]) across decades of age. Although there is an increase in relative adipose tissue volume (SAT_{rel} and VAT_{rel}) across decades, there is a decrease in SM_{rel} accompanied by an increase in SMFF. Sex-stratified median relative body composition measures and IQRs are provided in the tables below the plots. Q = quartile; rel = body composition measure relative to the sum of all body composition measures; SAT = subcutaneous adipose tissue; SM = skeletal muscle; SMFF = skeletal muscle fat fraction; VAT = visceral adipose tissue.

for epidemiologic studies or as a screening tool (3). Cardiometabolic disease guidelines suggest more direct measurement of adiposity using anthropometric metrics like WC and waist-to-hip ratio or dual-energy x-ray absorptiometry (32, 33). These measures are more closely related to abdominal adiposity than BMI but do not allow assessment of relative BC proportions (correlation to VAT-SAT ratio of ~0.1), suggesting that they may be proxies of total adiposity or size (34). The model used in this study enables direct measurement of BC compartments and relative proportions, which are shown here to be associated with cardiometabolic risk beyond BMI and WC.

The benefit of anthropometric metrics is their ease of use. Whole-body MRI is becoming increasingly popular as a direct-to-consumer screening tool but is not performed in routine clinical practice. Although we do not recommend specifically ordering whole-body MRI

Figure 2. Multivariable-adjusted spline curves for incident diabetes.

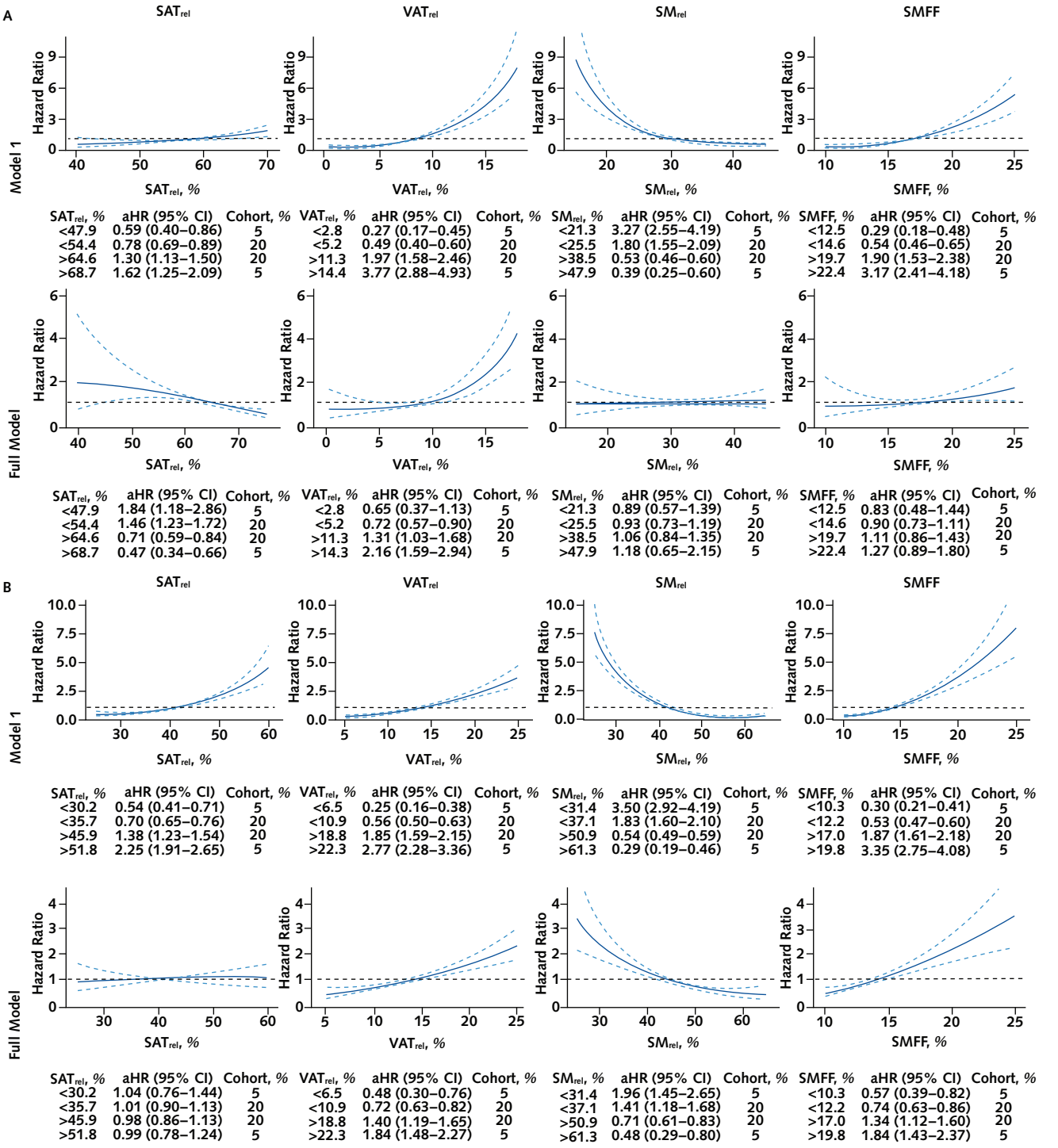

Sex-stratified multivariable-adjusted spline plots for females (*A*) and males (*B*) show the relationship between relative body composition measures and incident diabetes risk. The tables below each graph show the aHRs and the 95% CIs (*dark horizontal and blue dashed lines, respectively, in plots*) for the bottom and top 5% and 20% of the cohort. Model 1 was adjusted for age, prevalent hypertension, and smoking status. The full model was also adjusted for body mass index categories and waist circumference. aHR = adjusted hazard ratio; rel = body composition measure relative to the sum of all body composition measures; SAT = subcutaneous adipose tissue; SM = skeletal muscle; SMFF = skeletal muscle fat fraction; VAT = visceral adipose tissue.

Figure 3. Multivariable-adjusted spline curves for incident MACE.

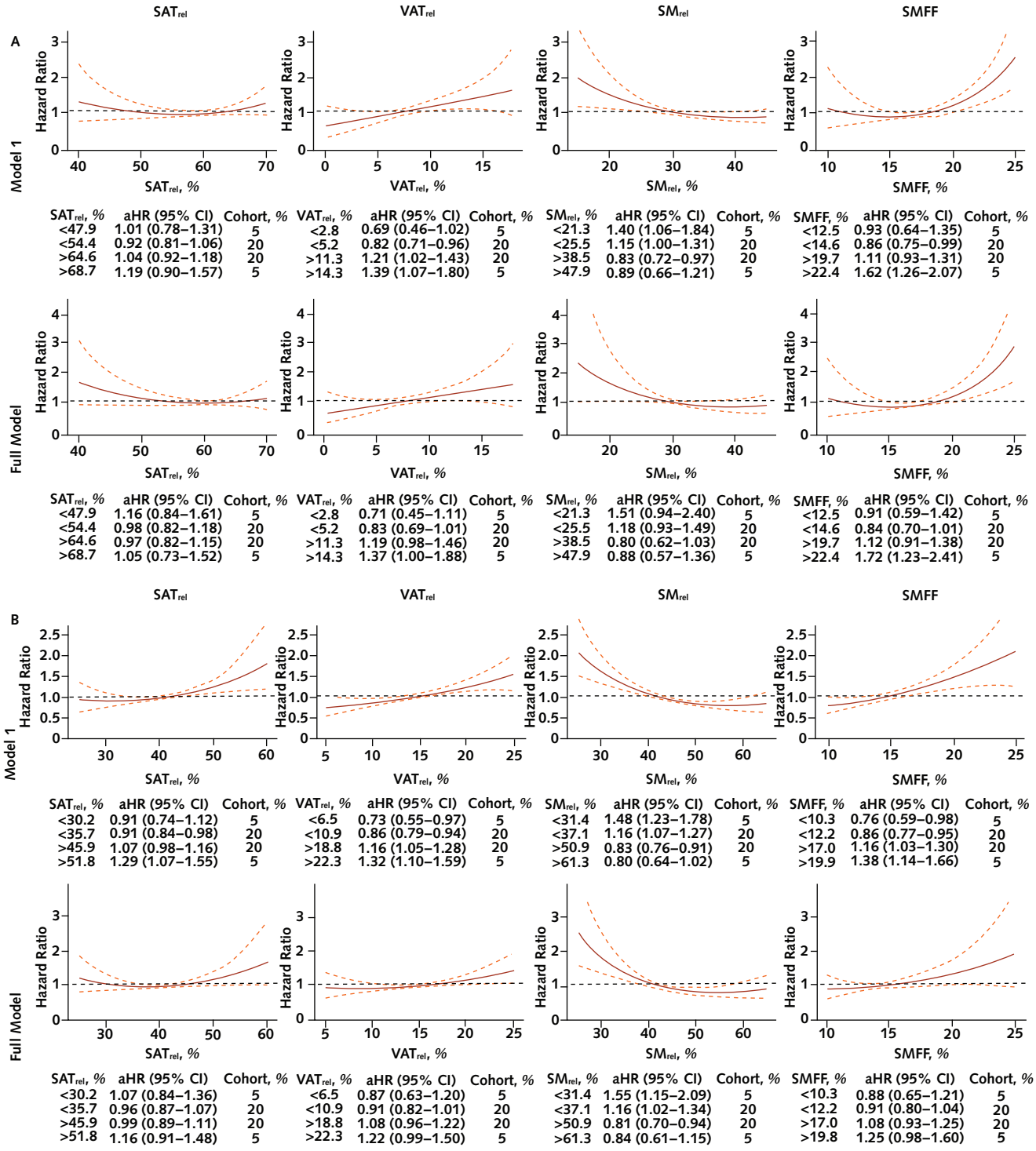

A, Model 1												
SAT_{rel}, %	aHR (95% CI)	Cohort, %	VAT_{rel}, %	aHR (95% CI)	Cohort, %	SM_{rel}, %	aHR (95% CI)	Cohort, %	SMFF, %	aHR (95% CI)	Cohort, %
<47.9	1.01 (0.78–1.31)	5	<2.8	0.69 (0.46–1.02)	5	<21.3	1.40 (1.06–1.84)	5	<12.5	0.93 (0.64–1.35)	5
<54.4	0.92 (0.81–1.06)	20	<5.2	0.82 (0.71–0.96)	20	<25.5	1.15 (1.00–1.31)	20	<14.6	0.86 (0.75–0.99)	20
>64.6	1.04 (0.92–1.18)	20	>11.3	1.21 (1.02–1.43)	20	>38.5	0.83 (0.72–0.97)	20	>19.7	1.11 (0.93–1.31)	20
>68.7	1.19 (0.90–1.57)	5	>14.3	1.39 (1.07–1.80)	5	>47.9	0.89 (0.66–1.21)	5	>22.4	1.62 (1.26–2.07)	5

A, Full Model												
SAT_{rel}, %	aHR (95% CI)	Cohort, %	VAT_{rel}, %	aHR (95% CI)	Cohort, %	SM_{rel}, %	aHR (95% CI)	Cohort, %	SMFF, %	aHR (95% CI)	Cohort, %
<47.9	1.16 (0.84–1.61)	5	<2.8	0.71 (0.45–1.11)	5	<21.3	1.51 (0.94–2.40)	5	<12.5	0.91 (0.59–1.42)	5
<54.4	0.98 (0.82–1.18)	20	<5.2	0.83 (0.69–1.01)	20	<25.5	1.18 (0.93–1.49)	20	<14.6	0.84 (0.70–1.01)	20
>64.6	0.97 (0.82–1.15)	20	>11.3	1.19 (0.98–1.46)	20	>38.5	0.80 (0.62–1.03)	20	>19.7	1.12 (0.91–1.38)	20
>68.7	1.05 (0.73–1.52)	5	>14.3	1.37 (1.00–1.88)	5	>47.9	0.88 (0.57–1.36)	5	>22.4	1.72 (1.23–2.41)	5

B, Model 1												
SAT_{rel}, %	aHR (95% CI)	Cohort, %	VAT_{rel}, %	aHR (95% CI)	Cohort, %	SM_{rel}, %	aHR (95% CI)	Cohort, %	SMFF, %	aHR (95% CI)	Cohort, %
<30.2	0.91 (0.74–1.12)	5	<6.5	0.73 (0.55–0.97)	5	<31.4	1.48 (1.23–1.78)	5	<10.3	0.76 (0.59–0.98)	5
<35.7	0.91 (0.84–0.98)	20	<10.9	0.86 (0.79–0.94)	20	<37.1	1.16 (1.07–1.27)	20	<12.2	0.86 (0.77–0.95)	20
>45.9	1.07 (0.98–1.16)	20	>18.8	1.16 (1.05–1.28)	20	>50.9	0.83 (0.76–0.91)	20	>17.0	1.16 (1.03–1.30)	20
>51.8	1.29 (1.07–1.55)	5	>22.3	1.32 (1.10–1.59)	5	>61.3	0.80 (0.64–1.02)	5	>19.9	1.38 (1.14–1.66)	5

B, Full Model												
SAT_{rel}, %	aHR (95% CI)	Cohort, %	VAT_{rel}, %	aHR (95% CI)	Cohort, %	SM_{rel}, %	aHR (95% CI)	Cohort, %	SMFF, %	aHR (95% CI)	Cohort, %
<30.2	1.07 (0.84–1.36)	5	<6.5	0.87 (0.63–1.20)	5	<31.4	1.55 (1.15–2.09)	5	<10.3	0.88 (0.65–1.21)	5
<35.7	0.96 (0.87–1.07)	20	<10.9	0.91 (0.82–1.01)	20	<37.1	1.16 (1.02–1.34)	20	<12.2	0.91 (0.80–1.04)	20
>45.9	0.99 (0.89–1.11)	20	>18.8	1.08 (0.96–1.22)	20	>50.9	0.81 (0.70–0.94)	20	>17.0	1.08 (0.93–1.25)	20
>51.8	1.16 (0.91–1.48)	5	>22.3	1.22 (0.99–1.50)	5	>61.3	0.84 (0.61–1.15)	5	>19.8	1.25 (0.98–1.60)	5

Sex-stratified multivariable adjusted spline plots for females (*A*) and males (*B*) show the relationship between relative body composition measures and incident MACE risk. The tables below each graph show the aHRs and the 95% CIs (*dark horizontal and orange dashed lines, respectively, in plots*) for the bottom and top 5% and 20% of the cohort. Model 1 was adjusted for age, prevalent hypertension, and smoking status. The full model was also adjusted for body mass index categories and waist circumference. aHR = adjusted hazard ratio; rel = body composition measure relative to the sum of all body composition measures; SAT = subcutaneous adipose tissue; SM = skeletal muscle; SMFF = skeletal muscle fat fraction; VAT = visceral adipose tissue.

to assess BC, a pragmatic clinical implementation may be an opportunistic screening strategy, where BC data are automatically extracted from routine clinical MRI or CT scans, regardless of their initial indication. A critical next step toward this paradigm is to test whether BC proportions extracted from common clinical scan regions (such as the liver or kidneys) produce estimates similar to those of our whole-body approach. If successful, this model could be implemented in the electronic medical record without disrupting established workflows to automatically quantify potentially prognostic BC measurements from routine MRI or CT scans that would otherwise be missed. Our model was trained on a T_1-weighted Dixon sequence, which is widely used in routine practice and is comparable to other commonly used T_1-weighted sequences (35).

Growing evidence suggests that BC plays a key role not only in cardiometabolic but also oncologic diseases to personalize risk estimation (36–38). In addition, BC could also play a crucial role in estimating treatment tolerability and risk for treatment-related toxicity. In this context, beyond defining excess adiposity, our DL model and relative BC profiles could be used as a measure of frailty or overall health to improve treatment decisions for accurate, personalized dosing of systemic drug therapies, including chemotherapy and immunotherapy (38–40).

This study has limitations. First, the study population is non-Hispanic White adults older than 45 years, and the results may not be generalizable to other demographic groups (18). A major challenge in obesity management is that BMI and WC require specific thresholds and have variable accuracy in identifying excess adiposity in people of different races or ethnicities. Magnetic resonance imaging has the potential to address this issue with direct measurement of BC (41); however, further testing is needed to determine whether the DL model is generalizable to diverse populations. We evaluated the DL segmentations on a relatively small testing cohort (50 participants from NAKO and 50 from UKB) and did not have repeated scans to assess test–retest reliability; however, Bland–Altman analysis showed that DL segmentations were robust despite the small testing cohort. Third, Dixon swap artifacts are common errors in routine clinical practice, meaning that a fat-only signal can be erroneously displayed in parts where a water-only signal is expected, resulting in incorrect Dixon-derived SMFF calculations (42, 43). Although we corrected swap artifacts in our study before SMFF extraction, this may be a barrier to the translation of SMFF into practice. Furthermore, future studies need to investigate whether the model is generalizable to non-Siemens scans and different field strengths. Fourth, granular information on smoking history (such as pack-years), physical activity, and socioeconomic status was not available for most of our cohort and may introduce residual confounding. Finally, we used thoracoabdominal SAT, VAT, and SM; however, fat location (for example, ectopic or gluteofemoral fat) may play different roles in conferring cardiometabolic risk. Future studies will focus on clinical or anatomical region–specific measurements to improve its clinical utility.

In conclusion, automated MRI-based BC analysis is accurate and feasible. Automated BC measurements are associated with cardiometabolic risk beyond BMI, WC, and traditional risk factors. After further validation in diverse populations, this approach may enable opportunistic assessment of BC from routine imaging to identify patients at high cardiometabolic risk.

From Department of Diagnostic and Interventional Radiology, University Medical Center Freiburg, Faculty of Medicine, University of Freiburg, Freiburg, Germany, and Cardiovascular Imaging Research Center, Department of Radiology, Massachusetts General Hospital and Harvard Medical School, Boston, Massachusetts (M.J.); Medical Physics, Department of Diagnostic and Interventional Radiology, Medical Center-University of Freiburg, Faculty of Medicine, University of Freiburg, and Department of Stereotactic and Functional Neurosurgery, Medical Center - University of Freiburg, Faculty of Medicine, University of Freiburg, Freiburg, Germany (M.R.); Department of Diagnostic and Interventional Radiology, University Medical Center Freiburg, Faculty of Medicine, University of Freiburg, Freiburg, Germany (H.R., F.B., J.W.); Department of Diagnostic and Interventional Radiology, University Medical Center Freiburg, Faculty of Medicine, University of Freiburg, Freiburg, Germany, and Institute of Epidemiology, Helmholtz Zentrum München, German Research Center for Environmental Health, Neuherberg, Germany (S.R.); and Cardiovascular Imaging Research Center, Department of Radiology, Massachusetts General Hospital and Harvard Medical School, Boston, Massachusetts (M.T.L., V.K.R.).

Note: Informed consent was obtained from all participants in the UK Biobank.

Acknowledgment: This research was conducted using the UK Biobank Resource under application number 80337. The authors thank all participants who took part in the NAKO and UKB studies and the staff of these research initiatives.

Financial Support: Dr. Jung was supported by the Deutsche Forschungsgemeinschaft (German Research Foundation) (518480401). Dr. Raghu was supported by Norn Group Longevity Impetus Grant NHLBI K01HL168231 and AHA Career Development Award 935176.

Disclosures: Disclosure forms are available with the article online.

Reproducible Research Statement: *Study protocol:* Not available. *Statistical code:* Available via GitHub at https://github.com/circ-ml/MRI-Body-Comp. *Data set:* The data from the UKB may be accessed and downloaded upon request in accordance with UKB policies from https://www.ukbiobank.ac.uk. Our body composition measures are available at https://www.ukbiobank.ac.uk.

Corresponding Author: Jakob Weiss, MD, University Medical Center Freiburg, Hugstetter Straße 55, 79106 Freiburg im Breisgau, Germany; e-mail, jakob.benedikt.weiss@uniklinik-freiburg.de.

Author contributions are available at Annals.org.

References

1. **Afshin A, Forouzanfar MH, Reitsma MB, et al; GBD 2015 Obesity Collaborators.** Health effects of overweight and obesity in 195 countries over 25 years. N Engl J Med. 2017;377:13-27. [PMID: 28604169] doi:10.1056/NEJMoa1614362
2. **GBD 2021 US Obesity Forecasting Collaborators.** National-level and state-level prevalence of overweight and obesity among children, adolescents, and adults in the USA, 1990–2021, and forecasts up to 2050. Lancet. 2024;404:2278-2298. [PMID: 39551059] doi:10.1016/S0140-6736(24)01548-4
3. **Rubino F, Cummings DE, Eckel RH, et al.** Definition and diagnostic criteria of clinical obesity. Lancet Diabetes Endocrinol. 2025;13:221-262. [PMID: 39824205] doi:10.1016/S2213-8587(24)00316-4
4. **Shepherd JA, Ng BK, Sommer MJ, et al.** Body composition by DXA. Bone. 2017;104:101-105. [PMID: 28625918] doi:10.1016/j.bone.2017.06.010
5. **Ross R, Neeland IJ, Yamashita S, et al.** Waist circumference as a vital sign in clinical practice: a Consensus Statement from the IAS and ICCR Working Group on Visceral Obesity. Nat Rev Endocrinol. 2020;16:177-189. [PMID: 32020062] doi:10.1038/s41574-019-0310-7
6. **Agrawal S, Klarqvist MDR, Diamant N, et al.** BMI-adjusted adipose tissue volumes exhibit depot-specific and divergent associations with cardiometabolic diseases. Nat Commun. 2023;14:266. [PMID: 36650173] doi:10.1038/s41467-022-35704-5
7. **NHS England.** Diagnostic Imaging Dataset 2012-13 Data. Accessed at https://www.england.nhs.uk/statistics/statistical-work-areas/diagnostic-imaging-dataset/diagnostic-imaging-dataset-2012-13-data-2 on 24 June 2024.
8. **NHS England.** Diagnostic Imaging Dataset 2023-24 Data. Accessed at https://www.england.nhs.uk/statistics/statistical-work-areas/diagnostic-imaging-dataset/diagnostic-imaging-dataset-2023-24-data on 24 June 2024.
9. **Organisation for Economic Co-operation and Development.** Magnetic Resonance Imaging (MRI) Exams. Accessed at https://www.oecd.org/en/data/indicators/magnetic-resonance-imaging-mri-exams.html?oecdcontrol-0ad85c6bab-var1=USA on 8 August 2025.
10. **Organisation for Economic Co-operation and Development.** Computed Tomography (CT) Exams. Accessed at https://www.oecd.org/en/data/indicators/computed-tomography-ct-exams.html?oecdcontrol-0ad85c6bab-var1=USA on 8 August 2025.
11. **Thomas EL, Bell JD.** Influence of undersampling on magnetic resonance imaging measurements of intra-abdominal adipose tissue. Int J Obes Relat Metab Disord. 2003;27:211-218. [PMID: 12587001] doi:10.1038/sj.ijo.802229
12. **Shen W, Chen J, Gantz M, et al.** A single MRI slice does not accurately predict visceral and subcutaneous adipose tissue changes during weight loss. Obesity (Silver Spring). 2012;20:2458-2463. [PMID: 22728693] doi:10.1038/oby.2012.168
13. **Faron A, Luetkens JA, Schmeel FC, et al.** Quantification of fat and skeletal muscle tissue at abdominal computed tomography: associations between single-slice measurements and total compartment volumes. Abdom Radiol (NY). 2019;44:1907-1916. [PMID: 30694368] doi:10.1007/s00261-019-01912-9
14. **Jung M, Raghu VK, Reisert M, et al.** Deep learning-based body composition analysis from whole-body magnetic resonance imaging to predict all-cause mortality in a large Western population. EBioMedicine. 2024;110:105467. [PMID: 39622188] doi:10.1016/j.ebiom.2024.105467
15. **Derstine BA, Holcombe SA, Ross BE, et al.** Optimal body size adjustment of L3 CT skeletal muscle area for sarcopenia assessment. Sci Rep. 2021;11:279. [PMID: 33431971] doi:10.1038/s41598-020-79471-z
16. **Sudlow C, Gallacher J, Allen N, et al.** UK Biobank: an open access resource for identifying the causes of a wide range of complex diseases of middle and old age. PLoS Med. 2015;12:e1001779. [PMID: 25826379] doi:10.1371/journal.pmed.1001779
17. **Bamberg F, Kauczor H-U, Weckbach S, et al; German National Cohort MRI Study Investigators.** Whole-body MR imaging in the German National Cohort: rationale, design, and technical background. Radiology. 2015;277:206-220. [PMID: 25989618] doi:10.1148/radiol.2015142272
18. **Littlejohns TJ, Holliday J, Gibson LM, et al.** The UK Biobank imaging enhancement of 100,000 participants: rationale, data collection, management and future directions. Nat Commun. 2020;11:2624. [PMID: 32457287] doi:10.1038/s41467-020-15948-9
19. **German National Cohort (GNC) Consortium.** The German National Cohort: aims, study design and organization. Eur J Epidemiol. 2014;29:371-382. [PMID: 24840228] doi:10.1007/s10654-014-9890-7
20. **Shulman GI.** Ectopic fat in insulin resistance, dyslipidemia, and cardiometabolic disease. N Engl J Med. 2014;371:1131-1141. [PMID: 25229917] doi:10.1056/NEJMra1011035
21. **Koh H, Hayashi T, Sato KK, et al.** Visceral adiposity, not abdominal subcutaneous fat area, is associated with high blood pressure in Japanese men: the Ohtori study. Hypertens Res. 2011;34:565-572. [PMID: 21228782] doi:10.1038/hr.2010.271
22. **Porter SA, Massaro JM, Hoffmann U, et al.** Abdominal subcutaneous adipose tissue: a protective fat depot? Diabetes Care. 2009;32:1068-1075. [PMID: 19244087] doi:10.2337/dc08-2280
23. **Souza ACDAH, Troschel AS, Marquardt JP, et al.** Skeletal muscle adiposity, coronary microvascular dysfunction, and adverse cardiovascular outcomes. Eur Heart J. 2025;46:1112-1123. [PMID: 39827905] doi:10.1093/eurheartj/ehae827
24. **Goodpaster BH, Bergman BC, Brennan AM, et al.** Intermuscular adipose tissue in metabolic disease. Nat Rev Endocrinol. 2023;19:285-298. [PMID: 36564490] doi:10.1038/s41574-022-00784-2
25. **Diaz-Canestro C, Pentz B, Sehgal A, et al.** Lean body mass and the cardiovascular system constitute a female-specific relationship. Sci Transl Med. 2022;14:eabo2641. [PMID: 36260693] doi:10.1126/scitranslmed.abo2641
26. **Golan R, Shelef I, Rudich A, et al.** Abdominal superficial subcutaneous fat: a putative distinct protective fat subdepot in type 2 diabetes. Diabetes Care. 2012;35:640-647. [PMID: 22344612] doi:10.2337/dc11-1583
27. **Chen P, Hou X, Hu G, et al.** Abdominal subcutaneous adipose tissue: a favorable adipose depot for diabetes? Cardiovasc Diabetol. 2018;17:93. [PMID: 29945626] doi:10.1186/s12933-018-0734-8
28. **Wee CC, Batch BC, Guallar E.** Staging obesity risk beyond body mass index: progress made but more to do. Ann Intern Med. 2025;178:1199-1200. [PMID: 40623309] doi:10.7326/ANNALS-25-02327
29. **Gilden AH, Catenacci VA, Taormina JM.** Obesity. Ann Intern Med. 2024;177:ITC65-ITC80. [PMID: 38739920] doi:10.7326/AITC202405210
30. **Dicker D, Karpati T, Promislow S, et al.** Implications of the European Association for the Study of Obesity's new framework definition of obesity: prevalence and association with all-cause mortality. Ann Intern Med. 2025;178:1065-1072. [PMID: 40623308] doi:10.7326/ANNALS-24-02547
31. **Aragaki AK, Manson JE, LeBlanc ES, et al.** Development and validation of body mass index-specific waist circumference thresholds in postmenopausal women: a prospective cohort study. Ann Intern Med. 2025;178:1073-1084. [PMID: 40623313] doi:10.7326/ANNALS-24-00713
32. **American Diabetes Association Professional Practice Committee.** 8. Obesity and weight management for the prevention and treatment of type 2 diabetes: Standards of Care in Diabetes–2024. Diabetes Care. 2024;47:S145-S157. [PMID: 38078578] doi:10.2337/dc24-S008

33. **Powell-Wiley TM, Poirier P, Burke LE, et al; American Heart Association Council on Lifestyle and Cardiometabolic Health; Council on Cardiovascular and Stroke Nursing; Council on Clinical Cardiology; Council on Epidemiology and Prevention; Stroke Council.** Obesity and cardiovascular disease: a scientific statement from the American Heart Association. Circulation. 2021;143:e984-e1010. [PMID: 33882682] doi:10.1161/CIR.0000000000000973

34. **Klarqvist MDR, Agrawal S, Diamant N, et al.** Silhouette images enable estimation of body fat distribution and associated cardiometabolic risk. NPJ Digit Med. 2022;5:105. [PMID: 35896726] doi:10.1038/s41746-022-00654-1

35. **Salari R, Ballard DH, Hoegger MJ, et al.** Fat-only Dixon: how to use it in body MRI. Abdom Radiol (NY). 2022;47:2527-2544. [PMID: 35583822] doi:10.1007/s00261-022-03546-w

36. **Bates DDB, Pickhardt PJ.** CT-derived body composition assessment as a prognostic tool in oncologic patients: from opportunistic research to artificial intelligence–based clinical implementation. AJR Am J Roentgenol. 2022;219:671-680. [PMID: 35642760] doi:10.2214/AJR.22.27749

37. **DeFreitas MR, Toronka A, Nedrud MA, et al.** CT-derived body composition measurements as predictors for neoadjuvant treatment tolerance and survival in gastroesophageal adenocarcinoma. Abdom Radiol (NY). 2023;48:211-219. [PMID: 36209446] doi:10.1007/s00261-022-03695-y

38. **Cespedes Feliciano EM, Chen WY, Lee V, et al.** Body composition, adherence to anthracycline and taxane-based chemotherapy, and survival after nonmetastatic breast cancer. JAMA Oncol. 2020;6:264-270. [PMID: 31804676] doi:10.1001/jamaoncol.2019.4668

39. **Falsarella GR, Gasparotto LPR, Barcelos CC, et al.** Body composition as a frailty marker for the elderly community. Clin Interv Aging. 2015;10:1661-1666. [PMID: 26527868] doi:10.2147/CIA.S84632

40. **Griggs JJ, Bohlke K, Balaban EP, et al.** Appropriate systemic therapy dosing for obese adult patients with cancer: ASCO guideline update. J Clin Oncol. 2021;39:2037-2048. [PMID: 33939491] doi:10.1200/JCO.21.00471

41. **Rao G, Powell-Wiley TM, Ancheta I, et al; American Heart Association Obesity Committee of the Council on Lifestyle and Cardiometabolic Health.** Identification of obesity and cardiovascular risk in ethnically and racially diverse populations: a scientific statement from the American Heart Association. Circulation. 2015;132:457-472. [PMID: 26149446] doi:10.1161/CIR.0000000000000223

42. **Kirchgesner T, Acid S, Perlepe V, et al.** Two-point Dixon fat-water swapping artifact: lesion mimicker at musculoskeletal T2-weighted MRI. Skeletal Radiol. 2020;49:2081-2086. [PMID: 32556469] doi:10.1007/s00256-020-03512-x

43. **Haueise T, Schick F, Stefan N, et al.** Analysis of volume and topography of adipose tissue in the trunk: results of MRI of 11,141 participants in the German National Cohort. Sci Adv. 2023;9:eadd0433. [PMID: 37172093] doi:10.1126/sciadv.add0433

Author Contributions: Conception and design: M. Jung, S. Rospleszcz, F. Bamberg, V.K. Raghu, J. Weiss.
Analysis and interpretation of the data: M. Jung, M. Reisert, H. Rieder, S. Rospleszcz, M.T. Lu, F. Bamberg, V.K. Raghu, J. Weiss.
Drafting of the article: M. Jung, S. Rospleszcz, V.K. Raghu, J. Weiss.
Critical revision for important intellectual content: M. Jung, S. Rospleszcz, M.T. Lu, F. Bamberg, V.K. Raghu, J. Weiss.
Final approval of the article: M. Jung, M. Reisert, H. Rieder, S. Rospleszcz, M.T. Lu, F. Bamberg, V.K. Raghu, J. Weiss.
Provision of study materials or patients: J. Weiss.
Statistical expertise: M. Jung, M. Reisert, S. Rospleszcz, V.K. Raghu, J. Weiss.
Obtaining of funding: M. Jung, M.T. Lu, F. Bamberg, J. Weiss.
Administrative, technical, or logistic support: M. Reisert, S. Rospleszcz, M.T. Lu, F. Bamberg, V.K. Raghu, J. Weiss.
Collection and assembly of data: M. Jung, M. Reisert, H. Rieder, V.K. Raghu, J. Weiss.